Relationship between Hydrophobic Interactions and Secondary Structure Stability for Trpzip β-Hairpin Peptides[†]

Takahiro Takekiyo,[‡,§] Ling Wu,[‡] Yukihiro Yoshimura,[§] Akio Shimizu,[||] and Timothy A. Keiderling*[,‡]

Department of Chemistry, University of Illinois at Chicago, 845 West Taylor Street, Chicago, Illinois 60607-7061, Department of Applied Chemistry, National Defense Academy, 1-10-20, Hashirimizu, Yokosuka, Kanagawa 239-8686, Japan, and Department of Environmental Engineering for Symbiosis Factory of Engineering, Soka University, 1-236 Tangi-cho, Hachioji, Tokyo 192-8577, Japan

Received October 22, 2008; Revised Manuscript Received December 26, 2008

ABSTRACT: The temperature-induced β-hairpin stabilities of selected mutations of the Trpzip1 peptide, S**W**T**W**EGNK**W**T**W**K (**WWWW**), have been investigated by electronic circular dichroism (CD), Raman, and FT-IR spectroscopies. The tryptophan (Trp) residues in the original Trpzip1 sequence were systematically substituted with tyrosine (Tyr) in different positions to test the impact of Trp interactions on the β-hairpin structure and stability. The CD intensity at ∼228 nm, which arises from Trp−Trp interactions (tertiary structure), and the amide I′ IR absorbance at ∼1635 cm^{-1} (secondary structure) have been measured over a range of temperatures to investigate the impact of Tyr substitution on β-hairpin thermal stability in Trpzip peptides. Mutation from Trp to Tyr in the Trpzip1 sequence reduces the extent of β-hairpin structure and monotonically decreases the β-hairpin stability of Trpzip1 mutant peptides with an increasing number of Tyr substitutions. Substituted Trpzip peptides with just one pair of Trp−Trp interactions close to either the terminal residues (WYYW) or the turn (YWWY) have similar stabilities. Comparison of conformational transitions monitored by CD and IR reveals them to have multistate behavior in which the temperature-induced disruption of the Trp−Trp interaction (tertiary structure) occurs at a lower temperature than the unfolding of the secondary structure.

Protein folding has been modeled as being dependent on the formation of segments of secondary structure and their assembly into globular structures as related by tertiary structure. Alternatively, tertiary interactions (hydrophobic collapse) have been proposed to initially condense the structure and facilitate formation of secondary structure. Understanding the order of the steps in such an assembly and the mechanism of each step has long been a major goal in biophysical studies. The primary segments are often characterized as helices and sheets, of which the former is a fairly well-defined continuous part of the sequence, but the latter additionally involves a tertiary interaction in stabilizing its secondary structure. The fundamental building block of sheets is the interaction of two extended strands in a cross-strand H-bonding arrangement that can bring sequential or totally nonrelated sequences in the protein together in antiparallel or parallel alignments. Thus, the driving force for forming a β-sheet structure can be local or dispersed in the sequence, and their balance has been the subject of many studies (*1*−*4*).

If sequential segments come together to form an antiparallel β-sheet structure in a protein, this structural element can be modeled using monomeric β-hairpin peptides, which consist of two β-strands linked by a short loop or turn. While arbitrary sequences abstracted from protein structures rarely form stable β-hairpins in aqueous solution, many researchers have shown that designed short peptides can fold to a β-hairpin structure in aqueous solution (*2, 5*−*8*). Thermodynamic studies of such short β-hairpin peptides can provide basic information for understanding the energies of fundamental peptide fragments important for protein folding which has been the topic of several previous studies (*4, 7, 9*−*31*).

The structural stability of β-hairpin peptides is mainly influenced by three interactions: hydrophobic interaction due to the side chain, turn stability, and interstrand hydrogen bonding (H-bond). The sequence dependence of hairpin stability has been studied by NMR,[1] CD, and IR methods as well as theoretical approaches (*5, 6, 37*). Turn structures can initiate hairpin formation by promoting cross-strand H-bonds close to the turn, but the most stable structures have added stability from side chain interaction in the strands, particularly through selective hydrophobic interaction. According to Cochran and co-workers (*32*−*36*) and Waters and co-workers (*5, 37, 38*), aromatic−aromatic interactions make a higher contribution to β-hairpin stability than do aliphatic−aromatic interactions.

In this work, we focus on the positional relationship between the aromatic−aromatic side chain interaction and the β-hairpin secondary structure stability. Cochran et al. (*32*)

[†] The work in the United States was supported in part by a grant from the National Science Foundation (CHE0710543, to T.A.K.).

* To whom correspondence should be addressed. Telephone: (312) 996-3156. Fax: (312) 996-0431. E-mail: tak@uic.edu.

[‡] University of Illinois at Chicago.

[§] National Defense Academy.

[||] Soka University.

[1] Abbreviations: Trpzip, tryptophan zipper; NMR, nuclear magnetic resonance; CD, circular dichroism; IR, infrared; FT, Fourier transform; TFA, trifluoroacetic acid.

10.1021/bi8019838 CCC: $40.75
Published on Web 01/27/2009

synthesized a series of hairpins termed the Trpzip peptides, which contain two cross-strand Trp−Trp pairs and have become the basis of many β-hairpin studies. The indole side chains of each Trp−Trp pair interact with each other by a pairwise perpendicular stacking arrangement, leading to increased thermal stability of the hairpin structure. Trpzip peptides are among the most stable designed β-hairpin peptides known and provide excellent platforms for investigation of the relationship between aromatic−aromatic interaction and secondary structure for β-hairpin stability. To isolate various interactions, we have mutated the sequence by systematic substitution of various Trp positions with Tyr using Cochran's Trpzip1 sequence as a template (*32*). For thermodynamic studies, Trpzip1 gives more complete conformational transitions in the accessible temperature range. These were then studied using IR, CD, and Raman spectroscopies and as a function of temperature for which the results were analyzed with a thermodynamic model.

Electronic circular dichroism (CD) spectroscopy can sometimes be useful for characterizing β-sheet secondary structure formation. However, in a peptide such as Trpzip, the strong CD peaks at ~213 and 228 nm are due to exciton coupling of $\pi-\pi^*$ transitions originating from the proximity of the indole side chains of the interacting Trp residues (*24, 32, 39*). The strong CD signal from the Trp indole rings at ~228 and ~213 nm overwhelms that originating from the amides in the β-sheet peptide structure (*40*) and acts as a monitor of Trp−Trp interaction. In addition, Raman spectroscopy can provide basic information about local interactions of residue side chains in peptides. Raman bands at ~1340 and ~1360 cm^{-1} are assigned to the Trp doublet resulting from the Fermi resonance between the fundamental band of an in-plane vibration (largely N═C stretching of the indole ring) and one or more combination bands of out-of-plane vibrations (*41*−*43*). The intensity ratio of the Trp doublet ($R = I_{1360}/I_{1340}$) changes with the environmental hydrophobicity of the Trp residue, thus reflecting tertiary structural changes for Trpzip1 peptides.

On the other hand, FTIR spectroscopy is a powerful technique for directly studying the β-sheet secondary structural change of peptides (*44*−*53*). The amide I′ vibration in FTIR spectra, primarily the C═O stretching mode of the amide linkage, appears in the region from 1620 to 1690 cm^{-1} with a frequency position and intensity pattern characteristic of the dominant secondary structure of the peptide. Therefore, this mode has long provided a monitor for sensing formation of β-sheet structures. The combination of CD and FTIR forms a complementary pair of techniques because the changes in the Trp exciton-coupled band at 213 and 228 nm in the CD report on the cross-strand (tertiary) side chain (Trp−Trp) interaction and the amide I′ band in the FTIR spectra has a shape and frequency that are dependent on the β-hairpin secondary structure. In a separately reported study, a similar comparison of aliphatic versus aromatic interactions, via modification of selected Trp residues to Val, was investigated using the Trpzip2 sequence (*40*).

MATERIALS AND METHODS

Peptide Synthesis and Purification. Trpzip1 (S**W**TW**W**EGNK**W**TW**W**K-NH_2) mutant peptides with Tyr (Y) substituted for Trp (W) at various positions, as indicated in Table 1 and Scheme 1, were synthesized using a PS3 peptide synthesizer (Protein Technologies Co.). A stepwise coupling of each amino acid was obtained using the standard solid-phase Fmoc coupling chemistry, with piperidine (PIP) and *N*-methylmorpholine (NMM) for Fmoc removal, 2-(1*H*-benzotriazol-1-yl)-1,1,3,3-tetramethyluronium (HBTU) as a coupling activation agent, and *N*,*N*-dimethylformamide (DMF) as a solvent. Four equivalents of amino acid and HBTU were used to synthesize these peptides on a 0.1 mmol scale. Once the synthesis was complete, the peptide was removed from the Fmoc-NH-SAL resin using a cleavage cocktail (80:12:6:2 TFA/thioanisole/1,2-ethanedithiol (EDT)/*m*-cresol mixture for 0.5−2 h). After removal of TFA by rotary evaporation, peptides were precipitated by addition of diethyl ether and then purified by HPLC (0.1% TFA in 95% acetonitrile/water). Peptide identification was confirmed by mass spectrometry (MS) on a Voyager-DE-PRO ABI time-of-flight mass spectrometer (TOF-MS).

Table 1: Peptide Sequences of Trpzip1 Mutant Peptides

abbreviation	sequence[a]	position substituted
WWWW	SWTWEGNKWTWK-NH_2	Trpzip1
WYWW	SWT**Y**EGNKWTWK-NH_2	Y4
WYYW	SWT**Y**EGNK**Y**TWK-NH_2	Y4Y9
YWWY	S**Y**TWEGNKWT**Y**K-NH_2	Y2Y11
YWYW	S**Y**TWEGNK**Y**TWK-NH_2	Y2Y9
YYYY	S**Y**T**Y**EGNK**Y**T**Y**K-NH_2	Y2Y4Y9Y11

[a] Bold and underlined residues represent the mutated positions.

Scheme 1: Schematic Structure of Trpzip1[a]

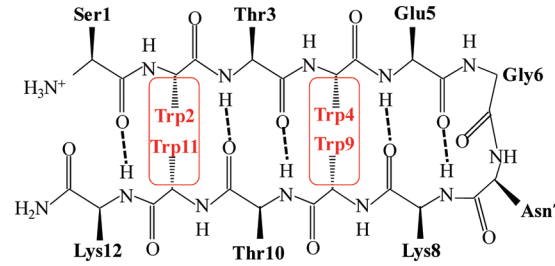

[a] The rectangles represent the dominant hydrophobic interactions (Trp2−Trp11 and Trp4−Trp9).

Circular Dichroism Measurements. For CD spectral measurements, peptide solutions were prepared at ~0.1 mg/mL (~0.06 mM) in 20 mM phosphate buffer (pH 6.7). Sample concentrations were determined using UV absorption (JASCO V-560) of Tyr and Trp (ε = 1197 M^{-1} cm^{-1} for Tyr and 5559 M^{-1} cm^{-1} for Trp at 280 nm). Thermal denaturation tests run on a Trpzip peptide showed a less than 2% change in absorbance on going from 278 to 363 K, demonstrating that these extinction values are valid for Trpzip1. CD spectra were initially recorded on a JASCO J-805 spectropolarimeter using a 0.1 cm path length cell. Thermal control of CD spectra used a Julabo F25HD thermal temperature bath under control of a JASCO program (JWJTC-484). For thermal conformational variation (unfolding) experiments, the temperature was increased from 278 to 348 K in 2 K increments and the single-wavelength CD response was monitored at 228 nm. Temperature variation studies of the full CD spectrum, measured every 5 K, were also run in Chicago (using a JASCO 810 with Neslab controller) under similar conditions to ensure the integrity of the samples and results. Typical spectra were accumulated

Table 2: Concentrations of Trpzip1 Mutant Peptides for IR Measurement

	concentration (mg/mL)		solubility limit (mg/mL)[a]	
peptide	pD 1.0	pD 7.0	pD 1.0	pD 7.0
WWWW (TZ1)	12.1	5.6	12.3	6.0
WYWW	10.0	6.0	10.4	6.2
WYYW (W2W11)	8.2	4.1	8.7	4.7
YWWY (W4W9)	7.9	3.8	8.3	4.4
YWYW (W4W11)	4.8	4.0	5.1	4.3
YYYY	3.2	3.9	3.8	4.1

[a] Concentration for noticeable aggregation.

at a scan rate of 50 nm/min with a 0.1 nm step resolution over the range of 185−260 nm, and eight scans were averaged for each spectrum. These latter data were used to obtain $[\theta]_{228}$ values, reported in molar ellipticity units (deg cm^2 dmol^{-1}), for the thermal analyses presented here.

FTIR and Raman Spectroscopic Measurements. Purified peptides were twice lyophilized against a 0.1 M DCl/D_2O solution (both DCl and D_2O from Sigma) to remove TFA counterions remaining from the peptide synthesis and cleavage and then redissolved in D_2O, neutralized with NaOD, and lyophilized again. Peptide solutions for IR measurement were prepared with a range of concentrations, 3.9−6.0 mg/mL for pD 7.0 in 20 mM phosphate buffer and 3.2−12.1 mg/mL for pD 1.0 in a 0.1 M DCl/D_2O solution adjusted to account for variations in solubility with different degrees of Tyr substitution as summarized in Table 2. These solutions were sealed in a demountable cell consisting of 25 mm CaF_2 windows separated by a 100 μm Teflon spacer and held in a brass compression ring.

FTIR spectra were measured using a DigiLab (Randolf, MA) FTS-60A spectrometer equipped with a DTGS detector. All spectra were collected at a resolution of 4 cm^{-1} with a zero-filling factor of 8. Temperature variation was accomplished with a homemade cell holder controlled from 278 to 363 K by flow from a bath (Neslab RTE 111). The experiments were realized by simultaneous execution of two independent programs (DigiLab Resolution Pro for spectral scan and NEScom for temperature ramp). The sample was heated in 5 K steps at 1 K/min followed by equilibration for 11 min and a 16 min data collect (940 scans coadded) before the next temperature step.

For Raman spectral measurements, peptide solutions were prepared using the same conditions as for the FTIR measurements. Spectra were recorded on a Raman spectrometer constructed at UIC that incorporated an Ar^+ laser (Coherent Innova 300) to excite the sample. Scattered light was collected at 90° with a simple (f/1) lens and refocused on the slit of a Jobin Yvon HR640 monochromator configured as a spectrograph with a CCD detector (Newton, Andor Technology) (*54, 55*). The sample was held in a quartz rectangular cell at 298 K. A 60 s exposure time with 300 mW excitation was used for each run, and 10 such spectral collections were accumulated and averaged. The amide I′ and Raman Trp doublet bands were fit with a Gaussian−Lorentzian mixing function using GRAMS (Galactic Industries) to investigate the static (298 K) folded state of Trpzip1 mutant peptides.

Thermal Analysis of Trpzip1 Peptides. The resulting IR and CD spectral amplitude variations with temperature at selected frequencies were fit to a two-state model. Normally,

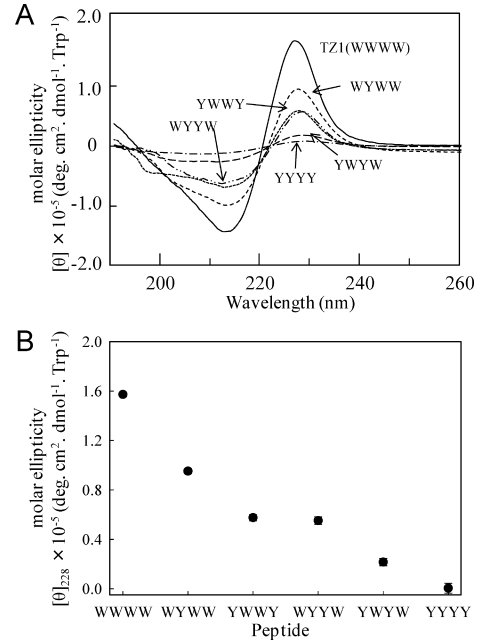

FIGURE 1: (A) CD spectra of Trpzip1 mutant peptides in aqueous solution at room temperature: WWWW (—), WYWW (---), YWWY (•••), WYYW (−••−), YWYW (−−−), and YYYY (−•−). (B) Variation in $[\theta]_{228}$ for Trpzip1 mutant peptides normalized to the number of Trp residues.

we used a linear folded and flat unfolded baseline with $\Delta C_p = 0$ (*21, 24*) because, after comparison with test calculations using other models, these constraints yielded improved fits both statistically and in terms of realistic parameters. (In these tests, the ΔC_p errors were much larger than the fit-determined values, indicating that $\Delta C_p \approx 0$.) The two-state model used for fitting the ECD ellipticity at 228 nm and the amide I′ absorbance at around 1635 cm^{-1} as a function of temperature is expressed as follows:

$$X = \frac{(m_F T + b_F) + b_U \exp\left[\left(\frac{\Delta H_m}{RT}\right)\left(\frac{1}{T_m} - \frac{1}{T}\right)\right]}{1 + \exp\left[\left(\frac{\Delta H_m}{RT}\right)\left(\frac{1}{T_m} - \frac{1}{T}\right)\right]} \quad (1)$$

where X is the experimental response in terms of ellipticity or absorbance, ΔH_m represents the enthalpy differences between the folded and unfolded states which we evaluated at the transition midpoint temperature (T_m), and the parameters m_F, b_F, and b_U represent the baseline parameters for the assumed linear and flat baselines of the folded (F) and unfolded (U) states, respectively.

RESULTS

Room-Temperature β-Hairpin Structure of Trpzip1 Mutant Peptides. At room temperature, the Trpzip1 hairpin is stable and gives rise to characteristic derivative-shaped CD in the far-UV region due to exciton coupling of the interacting Trp residues. On substitution of the various Trp positions with Tyr, this coupling is reduced, as shown in Figure 1. A single Tyr at position 4 (WYWW) drops the CD amplitude by a factor of more than 1.5, while two of them, in cross-strand positions, YWWY and WYYW, reduce it by a factor of ∼3 (as compared to WWWW), although the exciton coupling pattern remains dominant. The change in the negative CD

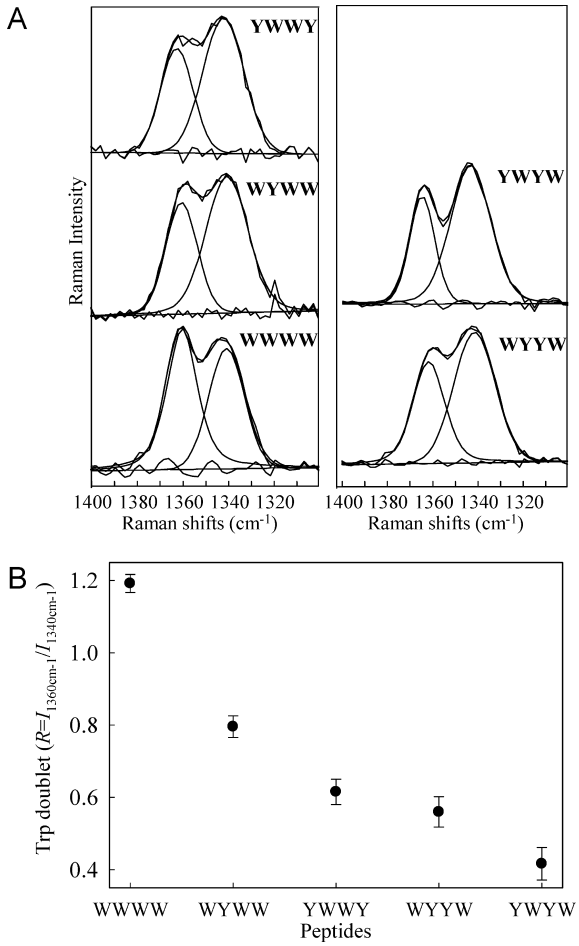

FIGURE 2: (A) Raman spectra in the Trp doublet region of Trpzip1 mutant peptides in aqueous solutions at room temperature. (B) Intensity ratios ($R = I_{1360}/I_{1340}$) of the Trp doublet as a function of Tyr substitution of the Trp in the Trpzip1 peptide.

band at 213 nm is consistent with that of the positive CD band at 228 nm which is expected for CD of an exciton-coupled pair of transitions. YWYW, which has Tyr at positions 2 and 9, is missing the CD couplet pattern due to loss of the cross-strand Trp−Trp interaction. Its CD intensity is not much higher than that for YYYY, with no Trp residues, implying there is much less coupling for this more separated pair of Trp side chains at positions W4 and W11. With loss of the cross-strand interaction in YWYW, in which Tyr breaks up each Trp−Trp pair, or with all Tyr in YYYY, the exciton pattern is lost and the residual CD pattern tends to reflect that of a disordered peptide.

In support of this interpretation of the CD results, the change in the Raman spectrum of the Trp doublet band resulting from the Fermi resonance of the indole ring vibrations is consistent with the weakened Trp−Trp interaction resulting from an increased level of Tyr substitution. Figure 2 compares the Raman Trp doublet spectra (Figure 2A) and their intensity ratios (R) (Figure 2B) for the Trpzip1-substituted peptides at 298 K. For this test, YYYY does not have a Trp doublet because all Trp residues were substituted. For comparison, the Raman spectra are normalized to a constant area to eliminate experimental variations. According to previous Raman Trp doublet studies of peptides and proteins, a large intensity ratio between the 1360 and 1340 cm^{-1} components of the Trp doublet ($R > 1$) is indicative of a hydrophobic Trp environment (*41, 57*). Thus, the decrease in the intensity ratio with an increased level of Tyr substitution indicates a decrease in the level of hydrophobic interaction, presumably due to more solvation of the Trp side chain accompanying decreased order. On the basis of the R value obtained for WWWW (from deconvolved component areas), a single Tyr at position 4 (WYWW) decreases the Trp doublet amplitude by a factor of 1.5, while for WYYW and YWWY, with Trp residues in cross-strand positions, it drops by a factor of 2 and for YWYW by a factor of 3. These R values of Trpzip1 peptides do qualitatively track those obtained with a simple Trp compound and with an acid-denatured protein, α-lactalbumin; however, since our ratios use fitted band intensities, they are not simply comparable to quantitative values reported in previous studies (*41, 57*).

On comparison of the variation of the CD and Raman results with Tyr substitution, the same trends are evident for the change in Trp−Trp interaction. Although Trp−Trp CD bands and Raman doublets for peptides (WYYW and YWWY) with one and two Tyr substitutions are weaker than those for WWWW, these peptides still have a clear Trp−Trp interaction, but YWYW does not. Moreover, WYYW and YWWY, which have Tyr in different positions, in pairs near the turn and near the termini, respectively, show similar Trp−Trp cross-strand interactions.

In the FTIR spectra, the intensities should reflect the concentration, so the spectra are normalized to a constant area. However, the shapes show a steady progression from Trpzip1 (WWWW), having a strong feature at ∼1635 cm^{-1} with a shoulder to a high wavenumber (∼1672 cm^{-1}), which is a form characteristic of a folded hairpin, to hairpins with an increasing level of Tyr substitution that have a broadened band shape whose maximum is shifted up in wavenumber. Efforts to fit the band shape as a sum of four components yielded the results shown in Figure 3A, which emphasizes the shift of the main intensity contribution from the lower- to central-frequency component in the overall band profile. Plots of the relative intensity of each component show a steady exchange between them which is consistent with a partial unfolding and destabilization of the secondary structure with loss of Trp−Trp interaction. However, the changes, unlike those seen in the CD and Raman spectra, are incremental with each substitution. In particular, the two cross-strand pairs at positions 2 and 11 (WYYW) and positions 4 and 9 (YWWY) show different intensity patterns, in contrast to their very similar Raman and CD profiles, and indicate that the Trp−Trp interaction closest to the turn has the stronger influence on hairpin stability.

To qualitatively estimate the relative degree of β-hairpin structure, we evaluated the changes in the amide I′ band peak area for the component fit at ∼1635 cm^{-1}, which largely corresponds to the β-strand contribution, as shown Figure 3B. The rank ordering of the relative β-strand peak areas (A_{1635}) is as follows: WWWW > WYWW > YWWY > WYYW > YWYW > YYYY, consistent with the CD and Raman results given above.

To further probe the Tyr role, we looked at the temperature dependence of the characteristic 1612 cm^{-1} band of Tyr, which arises from the phenol side chain vibration, in the various peptides. When a protein unfolds and its Tyr residues become exposed to the solvent, their absorption shifts to a higher wavenumber (*58, 59*). Consistent with this, the peak

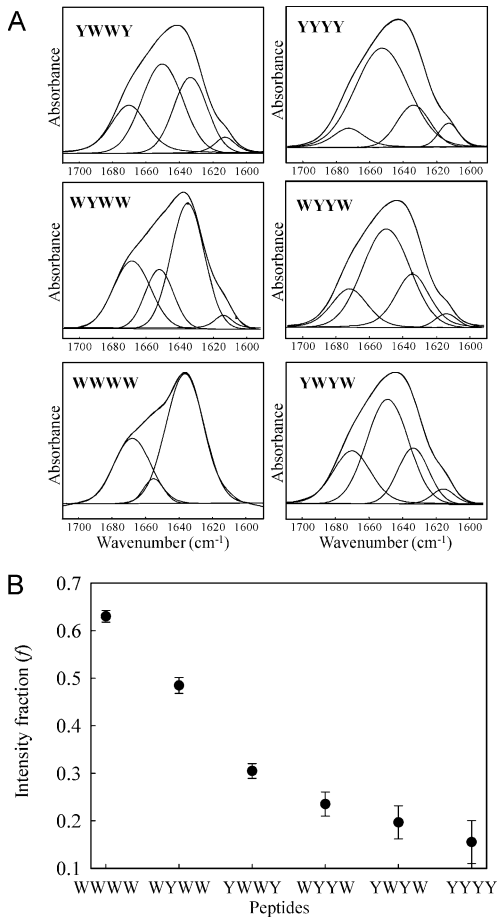

FIGURE 3: (A) FTIR spectra of the amide I′ region of Trpzip1 mutant peptides in aqueous solution at room temperature. The deconvolutions of FTIR spectra used a Gaussian−Lorentzian mixing function. The peak at ~1613 cm^{-1} is due to the side chain vibration of the Tyr residue. (B) Dependence on Tyr substitution of the fractional intensity (f) for the amide I′ component at 1635 cm^{-1}. The estimation of f used the relationship $f^{1635} = I^{1635}/(I^{1635} + I^{1643} + I^{1678})$, where I^{1635}, I^{1643}, and I^{1678} are the integrated intensities of the peaks at 1635 cm^{-1} (strand), 1643 cm^{-1} (disordered), and 1678 cm^{-1} (turn), respectively.

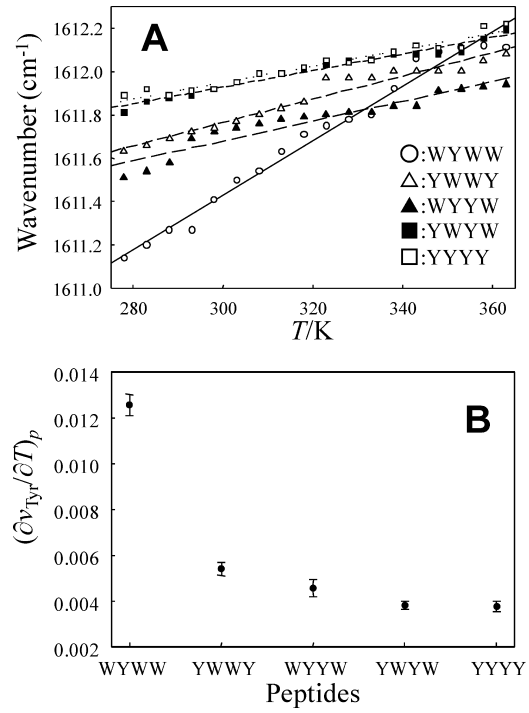

FIGURE 4: (A) Changes in the wavenumber of the maximum for the ~1612 cm^{-1} Tyr band in the Trpzip1 mutant peptides as a function of temperature. (B) Variation of the temperature dependence of the Tyr frequencies $(\partial\nu_{Tyr}/\partial T)_p$ with an increased level of Tyr substitution for the Trpzip1 mutant peptides. The straight lines (A) represent the results of the least-squares analysis, the slopes of which are the values plotted in panel B.

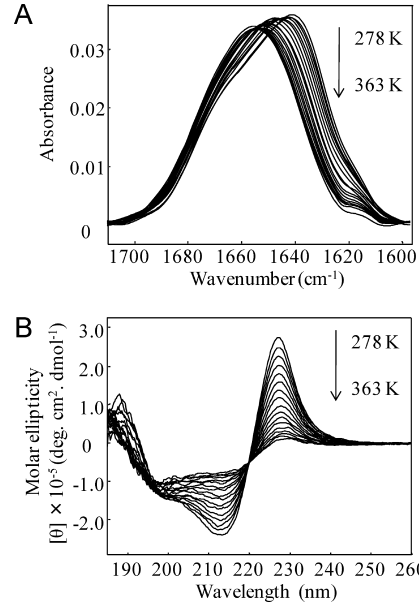

FIGURE 5: Typical examples of temperature variation of (A) FTIR and (B) CD spectra obtained for the Trpzip1 mutant peptides (shown here for YWWY) in aqueous solution.

at ~1612 cm^{-1} in all peptides shifts higher with increasing temperature as shown in Figure 4A. Thus, the wavenumber shift of the peak at ~1612 cm^{-1} seems to reflect the strength and hydrophobic shielding developed by the Tyr−Trp and Tyr−Tyr interactions (*60*). To quantitatively discuss the extent of temperature-induced frequency shift of the peak at ~1612 cm^{-1}, the temperature dependence for the peak at ~1612 cm^{-1}, $(\partial\nu_{Tyr}/\partial T)_p$ or the slope (Figure 4B), is used as a characterization. The value of $(\partial\nu_{Tyr}/\partial T)_p$ for WYWW is the largest of all the Tyr-modified Trpzip1 peptides. The value of $(\partial\nu_{Tyr}/\partial T)_p$ for YWWY is slightly larger than that for WYYW, while YWYW and YYYY exhibit almost the same values. The rank order of $(\partial\nu_{Tyr}/\partial T)_p$ values for the Trpzip1 mutants basically shows the same behavior patterns that were found with the CD and Raman results.

Thermal Unfolding of Trpzip1 Mutant Peptides. To further assess the impact of mutation from Trp to Tyr on β-hairpin stability, we measured the temperature dependences of A_{1635} and $[\theta]_{228}$ for the Trpzip1 mutant peptides as shown in panels A and B of Figure 5. In the CD spectra, the magnitudes of the strong negative−positive Trp−Trp exciton-coupled bands at ~213 and 228 nm decrease with an increase in temperature from 278 to 363 K, while a weak negative band at ~198 nm appears. These changes correlate to disruption of the Trp−Trp interaction for these Trpzip1 peptides with an increase in temperature. Similarly, the IR absorbance maximum peak of the Trpzip1 peptides shifts to higher frequency, decreases in intensity, and broadens with an increase in temperature from 278 to 363 K, consistent with loss of the cross-β-strand interaction. The thermal IR results (secondary structure) are consistent with the thermal CD results (Trp−Trp interaction); however, the IR spectra do not have an isosbestic

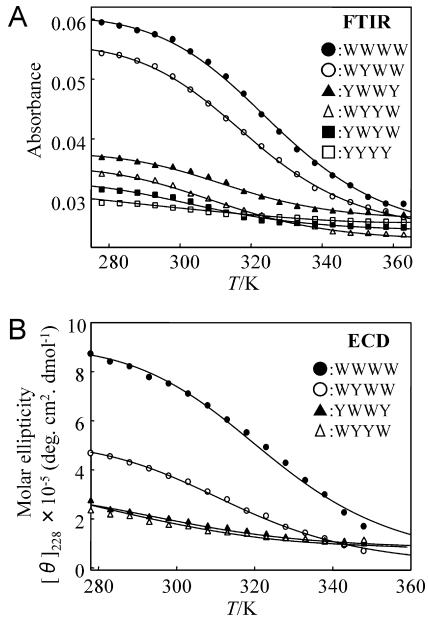

FIGURE 6: Fit of the changes for β-hairpin unfolding monitored as (A) the amide I′ absorbance at ~1635 cm^{-1} and (B) the molar ellipticity at 228 nm for Trpzip1 mutant peptides, under conditions where the thermal changes are reversible. Thermodynamic parameters were determined using a two-state fitting model.

point, while the CD does have an isodichroic point. Despite this indication of a deviation from two-state behavior, the CD and IR spectra were analyzed as described above. Thermodynamic parameters (T_m, ΔH, and ΔS) were determined in terms of the temperature dependences of $[\theta]_{228}$ and A_{1635} using a two-state model with linear folded and flat unfolded baselines where $\Delta C_p = 0$ (eq 1). Attempts to use other models resulted in much larger errors for the fit, and fits including ΔC_p gave values of zero within the fitting error.

Panels A and B of Figure 6 show the thermal equilibrium curves for the Trpzip1 peptides as obtained from the changes in A_{1635} and $[\theta]_{228}$, respectively. The T_m values determined by IR and CD spectra shift to lower temperature with an increased level of Tyr substitution which would be consistent with a steady decrease in stability as shown in Table 3. The data result in the following rank ordering of T_m for secondary structure (IR) and Trp−Trp interaction (CD): WWWW > WYWW > YWWY > WYYW > YWYW > YYYY. Although the T_m values of WWWW for CD and IR are similar, with an increased level of Tyr substitution they differ. The result is that the T_m for secondary structure (IR) is higher than that for Trp−Trp interaction (CD), and the T_m difference (ΔT_m) between the secondary structure and Trp−Trp interaction stabilities becomes larger with an increased level of Tyr substitution. In other words, the disruption of the aromatic−aromatic interaction associated with β-hairpin formation in the Trpzip1 peptides is easier, i.e., lower T_m, than the unfolding of secondary structure and becomes more so with an increased level of Tyr substitution. Such behavior again suggests that the process cannot be a simple two-state transition but must be at least stepwise.

The thermodynamic parameters echo this pattern, so that the ΔH and ΔS values for loss of secondary structure and of Trp−Trp interaction decrease with the same pattern: WWWW > WYWW > YWWY > WYYW > YWYW > YYYY. From comparing ΔH and ΔS for WYYW and YWWY, as determined by CD, the W4−W9 and W2−W11 interactions appear to be similar, but the W4−W9 interaction is slightly more enthalpically stable and is entropically more favorable than the W2−W11 interaction. This result is consistent with the ΔH and ΔS values determined by IR, reflecting their impact upon the secondary structure.

DISCUSSION

Effect of Tyr Substitution on the β-Hairpin Structure of Trpzip1 Peptides. Our results using a systematic mutation of the Trpzip1 sequence show that the Trp−Trp interaction is the key element of the unique stability for these peptides. For this study, we have substituted Tyr for Trp and destabilized the peptide secondary structure by weakening the hydrophobic interaction of the side chains. A representation of the Trp side chains from the Trpzip1 NMR structure of Cochran et al. (*32, 33*) is shown in Figure 7. Turning to the CD and Raman results, we find the molar ellipticity at 228 nm ($[\theta]_{228}$) and the Trp doublet intensity ratio (R), which both correlate to the Trp−Trp interaction, have the same stability ordering (WWWW > WYWW > YWWY > WYYW) for Trpzip1 mutant peptides. Because YWYW and YYYY do not have a strong positive CD peak at ~228 nm and have a small R value for the Raman Trp doublet, this implies that YWYW does not have a significant Trp4−Trp11 cross-strand interaction, due to either separation or partial unfolding. From IR results, the value of A_{1635} for WYWW is larger than that for WYYW. If WYWW were just missing the Trp9−Trp11 interaction, the value of A_{1635} for WYWW should be the same as that for WYYW. This comparison shows the level of β-hairpin partial unfolding in WYWW increases for WYYW and consequently suggests that a Trp−Tyr interaction is more stabilizing than a Tyr−Tyr interaction.

As described above, the $(\partial\nu_{Tyr}/\partial T)_p$ value for the temperature-dependent shift of the Tyr IR peak at ~1612 cm^{-1} for YWWY is slightly larger than that for WYYW, while YWYW and YYYY had almost the same values. All of these are much smaller than that for WYWW, which demonstrates again that the mixed side chain, Tyr4−Trp9 interaction has significant hydrophobic character and stabilizes the hairpin. [While the exciton band at 228 nm and Trp doublet ratio (R) of WYWW may be enhanced due to a weak Tyr4−Trp9 interaction, added β-hairpin stability from this interaction may also be the cause. These are difficult to separate.] On the basis of these results and earlier studies, the Trp−Trp pair clearly has the strongest interaction promoting β-hairpin stability, the Tyr−Trp pair has less, and the Tyr−Tyr interaction apparently has the weakest contribution. Comparison of CD, Raman, and IR results for WYYW with those for YWWY shows the values of $[\theta]_{228}$, R, and A_{1635} for YWWY, which has its Trp−Trp interaction close to the turn region, are larger than those for WYYW, having the Trp−Trp interaction closer to the termini. This additionally is consistent with the WYYW versus YWWY $(\partial\nu_{Tyr}/\partial T)_p$ comparison noted above. Of these, the IR difference (due only to secondary structure contribution) is the largest, and the CD (purely Trp−Trp interaction) is the smallest. While the Trp−Trp interaction is a dominant structure stabilizing factor, its impact on the hairpin is greater if it is closer to the tight turn, aiding formation of what is apparently a strained conformation.

Table 3: Thermodynamic Quantities for Trpzip1 Mutant Peptides in Aqueous Solutions Using the Two-State Fitting Model[a]

	T_m (K)		ΔH (kcal/mol)		ΔS (cal mol^{-1} K^{-1})	
peptide	FTIR	CD	FTIR	CD	FTIR	CD
WWWW	325.1 ± 1.2	323.0 ± 0.6	15.8 ± 0.8	12.1 ± 0.4	48.5	37.6
WYWW	319.5 ± 0.9	314.0 ± 1.3	13.6 ± 0.9	11.4 ± 0.3	42.5	36.4
YWWY	314.1 ± 0.7	299.2 ± 0.8	12.6 ± 0.9	9.5 ± 0.3	41.4	31.8
WYYW	311.8 ± 1.9	297.5 ± 1.2	12.2 ± 0.5	9.1 ± 0.4	38.9	30.6
YWYW	305.1 ± 1.5	−	11.2 ± 0.8	−	36.7	−
YYYY	303.4 ± 1.7	−	10.5 ± 1.3	−	34.6	−

[a] The fits assumed linear (folded) and flat (unfolded) baselines and $\Delta C_p = 0$.

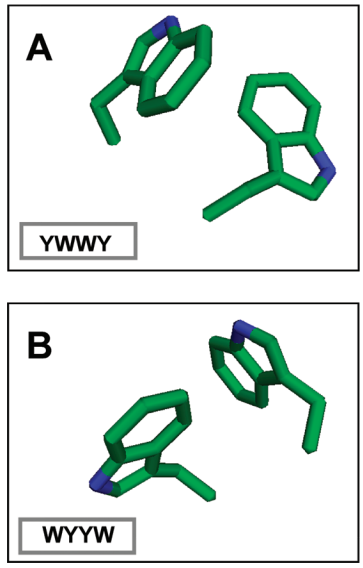

FIGURE 7: Comparison of Trp−Trp interaction for (A) W4W9, the inner cross-strand coupled pair by the turn, and (B) W2W11, the outer pair. Geometries were derived from the Trpzip1 NMR structure of Cochran et al. (*32, 33*).

Table 4: $\Delta\Delta H$ and $\Delta\Delta S$ for Trpzip1 Mutant Peptides

	secondary structure (IR)		tertiary structure (CD)	
peptide mutation	$\Delta\Delta H$ (kcal/mol)	$\Delta\Delta S$ (cal mol^{-1} K^{-1})	$\Delta\Delta H$ (kcal/mol)	$\Delta\Delta S$ (cal mol^{-1} K^{-1})
WWWW → WYWW	−2.2	−6.0	−0.7	−1.2
WYWW → WYYW	−1.0	−1.1	−1.9	−4.6
WYWW → YWWY	−1.4	−3.6	−2.3	−5.8

The data we have developed indicate an underlying multistate folding mechanism, but comparison of the results of analysis with a two-state thermodynamic model can still be qualitatively informative in terms of trends found in the parameters derived. The relative ordering of the thermodynamic quantities, T_m, ΔH, and ΔS, also supports this analysis in that the fact that T_m and ΔH decrease with an increased level of Tyr substitution indicates reduced stability. The Trp → Tyr substitution can be viewed as destabilizing the β-hairpin structure for Trpzip1 peptides, even though the Tyr−Trp interaction is stabilizing, as compared to no side chain interactions, and Tyr alone would offer shielding of the backbone from "solvent". Further analysis is possible by use of $\Delta\Delta H$ and $\Delta\Delta S$ values comparing thermodynamic changes accompanying various single-residue mutations, comparing WWWW → WYWW with WYWW → WYYW, as determined by CD and IR and shown in Table 4. That these are different is a measure of the Trp−Tyr interaction in comparison with the Trp−Trp and Tyr−Tyr interactions. The progress from WWWW to WYWW to WYYW shows a larger $\Delta\Delta H$ for the change from the Trp−Trp pair to the Trp−Tyr pair than from the Trp−Tyr pair to the Tyr−Tyr pair, as judged from secondary structure stability (IR), again indicating that the Trp−Trp interaction is special, imparting more structural stability than a simple additive substitution of Trp into the Tyr−Tyr pair would imply. If the Trp−Trp pair were not a unique interaction, $\Delta\Delta H$ and $\Delta\Delta S$ from WWWW to WYWW should be consistent with those from WYWW to WYYW. The tertiary stability changes are more complex, and additional relationships cannot be derived from the YYYY to YWYW comparison because these structures do not have a sufficiently characteristic response, in terms of CD band profile.

Comparison with Other β-Hairpin Peptides. The cross-strand aromatic residue interactions in hairpin peptides induce stabilization of the β-hairpin structure (*37, 38, 58*). This study showed that systematic Tyr substitution for Trp in the Trpzip1 peptide decreases the β-hairpin stability. This finding is consistent with various results from other laboratories. Cochran et al. (*32*) developed the Trpzip (TZ) structures by the introduction of two Trp−Trp cross-strand pairs to enhance β-hairpin stability. They did a comparative analysis of the thermal stability for TZ4, TZ5, and TZ6, which have four, two, and three Trp residues with WWWW, WYFW, and WWWV hydrophobic interaction patterns, respectively, coupled with a turn sequence taken from the B1 domain of *streptococcal* protein G, called the GB1 peptide (GE**W**T**Y**-DDATKT**F**T**V**TE) (*7, 32, 61*). Of these, TZ4 (WWWW) had the highest thermal stability. The thermal stability of TZ5 (WYFW) is slightly greater than that of TZ6 (WWWV), suggesting that in this system the added enthalpic stability due to a Trp−Trp interaction close to the turn sequence has slightly less impact on the hairpin than for one closer to the termini. Trpzip1 (WWWW) has the highest thermal stability of the peptides studied here, which is consistent with Trpzip peptides related to the GB1 peptide. However, the thermal stabilities of the Trp−Trp interaction closer to the turn as compared to the termini for Trpzip1 peptides are different from the case of TZ5 (WYFW) and TZ6 (WWWV).

In a separate study, Wu et al. (*40*) investigated the thermal stability of related Trpzip2 mutant peptides with Val substituted for Trp (yielding analogous WVVW and VWWV hydrophobic patterns) using IR and CD spectroscopies and confirmed their geometries by obtaining NMR structures. The CD patterns qualitatively follow those reported here and have been shown, by use of time-dependent DFT calculations, to be consistent with the edge-to-face pairwise geometry of the pairs of Trp indole rings (*39*). With Val substitution, the secondary structure thermal stability and degree of Trp−Trp interaction for TZ2(VWWV) are higher than those of TZ2 (WVVW), again showing that the Trp−Trp interaction near the turn in Trpzip2 peptides is stronger than that near the

termini. This order is consistent with the present, Tyr-perturbed TZ1 results and opposite the TZ5 (WYFW)−TZ6 (WWWV) relationship, which may reflect a difference in the tight β-turn geometry in TZ1 versus the larger loop characteristic of the GB1 peptide. (Clearly, more changes than just the W substitution occur between TZ5 and TZ6, but if we assume that W−W interaction is highly dominant, as seen in our studies, this comparison with WYYW is at least qualitatively valid.) From a comparison of our results with those of Wu et al. (*40*), the hydrophobic interaction of WYYW and YWWY should be stronger than that of TZ2 (WVVW) and TZ2 (VWWV). However, T_m values for thermal transitions of the secondary structure and the Trp−Trp interaction for TZ2 (WVVW) and TZ2 (VWWV) are higher than those for WYYW and YWWY. This is due to the difference in turn stability between the Trpzip1 (Gly−Asn) and Trpzip2 (Asn−Gly) sequence (their only difference), further demonstrating the interplay between hydrophobicity and turn stability. The Trp−Trp interaction in TZ2 (VWWV) has the same geometry as in TZ2, and as that in TZ1 (Figure 7A) as determined by comparison of the respective NMR structures (*40*), and, given the consistent CD results, implies that the edge-to-face structure is maintained in all these mutants.

Pastor et al. (*62*) reported that the aliphatic−aromatic cross-strand interaction is preferred for the hairpin stability with the MBH12 peptide, but aromatic−aromatic interactions seem to be preferred at non-hydrogen bonding (NHB) positions in models with different turn structures. A number of studies by Waters and co-workers (*5, 37, 38, 63*) have shown that the Trp−Trp interaction is much stronger than that for other hydrophobic interacting residues. On the basis of these results, the hydrophobic interaction for β-hairpin stability can be summarized as being strongly dependent on both the turn structure and the characteristics of the amino acid residues composing the hydrophobic cluster.

Thermodynamic Stability of β-Hairpin Structure of Trpzip1 Peptides. Opening the hairpin or unfolding the structure implies a loss of intramolecular hydrogen bond (H-bond) stability. Its net impact on the energetics is difficult to judge due to the tradeoff with H-bonding to the solvent and in terms of stability due to entropy gain. Generally, the enthalpy of H-bond formation in aqueous solution is ∼1.5 kcal/mol (*64*−*66*). Our thermal data should reflect this at some level if the hydrophobic loss is correlated to unfolding of the secondary structure. From the FTIR analyses, $\Delta\Delta H$ for a change from WWWW to WYWW is −2.8 kcal/mol, from WWWW to YWWY is −3.7 kcal/mol, from WWWW to WYYW is −4.6 kcal/mol, from WWWW to YWYW is −4.7 kcal/mol, and from WWWW to YYYY is −5.6 kcal/mol. If these $\Delta\Delta H$ values represented just a change in H-bond enthalpy, they would correspond to change of approximately 1.9 (WYWW), 2.5 (YWWY), 3.0 (WYYW), 3.1 (YWYW), and 3.7 (YYYY) intramolecular H-bonds, respectively. In such a model, the maximum number of peptide H-bonds would be 5 and, thus, YYYY would be nearly fully unfolded, consistent with the spectral band shapes seen experimentally, but WYYW, YWWY, and YWYW would be about the same, with residual H-bonds left between the strands as suggested by our IR results. Our isotopic labeling work and MD studies on Trpzip2 peptides suggest that these residual H-bonds are between the central residues, rather than at the termini or turn (*24, 30*), which is reflected in other MD studies (*67*).

The values of enthalpy change per residue (ΔH res^{-1}) accompanying hairpin unfolding of Trpzip1 mutant peptides as obtained by IR analysis are 1.31 kcal/mol for WWWW, 1.13 kcal/mol for WYWW, 1.05 kcal/mol for YWWY, 1.02 kcal/mol for WYYW, 0.93 kcal/mol for YWYW, and 0.88 kcal/mol for YYYY, suggesting a value of ΔH res^{-1} for Trpzip1 peptides of ∼1.0 kcal/mol. According to numerous studies of the helix−coil transition of alanine-rich peptides, the ΔH res^{-1} accompanying the helix−coil transition is ∼1.0 kcal/mol (*68*−*72*). Moreover, the ΔH res^{-1} accompanying the β-hairpin unfolding of the GB1 peptide is also 1.0 kcal/mol (*19*). Both of these are consistent with that accompanying β-hairpin unfolding of Trpzip1 mutant peptides. Reported values for ΔS res^{-1} accompanying hairpin unfolding and helix−coil transitions are 3.6 and 2.7 cal mol^{-1} K^{-1}, respectively, which are also close to the values we obtained for ΔS res^{-1} of Trpzip1 mutant peptides (ΔS res^{-1} ∼ 2.9−4.0 cal mol^{-1} K^{-1}). From these data, the values of ΔH and ΔS per residue for unfolding peptides appear to be ∼1.0 kcal/mol per residue and ∼3.0 cal mol^{-1} K^{-1} per residue, respectively. These admittedly selective results mean that the thermodynamic quantities for unfolding of peptides are roughly independent of the sequence details and secondary structure.

On the other hand, according to the thermodynamic studies of globular proteins by Privalov et al. (*73*), the average ΔH and ΔS per residue for globular proteins are 1.2 kcal/mol and 17.4 cal mol^{-1} K^{-1}, respectively. Thus, the ΔH value for protein unfolding is almost consistent with that of peptide unfolding, but the ΔS value is much higher. This inconsistency might arise from the relative sizes of proteins and peptides. In Trpzip as well as helical peptides, the relatively small size exposes the entire molecule to water, while in the larger, folded protein, there will be more steric inhibition for unfolding. Thus, the ΔS inconsistency may reflect the high degree of order in globular proteins as compared to these hairpins. Cochran et al. (*32*) also pointed out this difference. Another explanation may be that the Trp side chains in Trpzip peptides are in a relatively fixed geometry because of the strong edge-to-face interaction of Trp pairs. This should have resulted in a high ΔS for the Trpzip peptides. However, on the basis of our experimental data published here, we cannot discriminate between these possibilities. One test of its source would be measurement of ΔS for similar hairpin peptides without strong Trp−Trp interactions, such as for the Gellman-designed peptides (*2, 18, 20, 23*), to see if their ΔS res^{-1} values are comparable.

CONCLUSION

The β-hairpin thermal stabilities of the Trpzip1 peptides as modified by Trp → Tyr substitution have been investigated using CD, Raman, and IR spectroscopies. The Tyr substitution in Trpzip1 peptides induces a decrease of β-hairpin structural stability, yet weak interaction of Tyr with Trp may still contribute to WYWW and YWYW stabilities. The Trp−Trp pair forms the dominant hydrophobic interaction stabilizing the β-hairpin structure in the Trpzip1 peptide. Comparison with other turn sequences, such as those in the Trpzip2 and GB1 peptides, showed that there is a balance

between turn stability and cross-strand hydrophobic interaction in promoting β-hairpin stability. Thus, hydrophobicity of residues is not the only factor in stabilizing formation of these hairpins. Further studies on β-hairpin peptides exploring variables such as pressure effects and other aromatic residue substitutions will help us in understanding more details of β-hairpin stability.

ACKNOWLEDGMENT

We are grateful for access to useful computational results before publication from Petr Bour and Anjan Roy from TD-DFT calculations of the CD for pairs of Trp residues.

REFERENCES

1. Chitnumsub, P., Fiori, W. R., Lashuel, H. A., Diaz, H., and Kelly, J. W. (1998) The nucleation of nomomeric parallel β-sheet like structures and their self-assembly in aqueous solution. *Bioorg. Med. Biol. 7*, 39–59.
2. Gellman, S. H. (1998) Minimal model systems for β-sheet secondary structure in proteins. *Curr. Opin. Chem. Biol. 2*, 717–725.
3. Nesloney, C. L., and Kelly, J. W. (1996) Progress towards understanding β-sheet structure. *Bioorg. Med. Chem. 4*, 739–766.
4. Streicher, W. W., and Makhatadze, G. I. (2006) Calorimetric evidence for a two-state unfolding of the β-hairpin peptide Trpzip4. *J. Am. Chem. Soc. 128*, 30–31.
5. Hughes, R. M., and Waters, M. L. (2006) Model systems for β-hairpins and β-sheets. *Curr. Opin. Struct. Biol. 16*, 514–524.
6. Cheng, R. P., Gellman, S. H., and DeGrado, W. F. (2001) β-Peptides: From structure to function. *Chem. Rev. 101*, 3219–3232.
7. Muñoz, V., Thompson, P. A., and Hofrichter, J. (1997) Folding dynamics and mechanism of β-hairpin formation. *Nature 390*, 196–199.
8. Tsai, J. H., Waldman, A. S., and Nowick, J. S. (1999) Two new-β-strand mimic. *Bioorg. Med. Biol. 7*, 29–38.
9. Du, D., Tucker, M. J., and Gai, F. (2006) Understanding the mechanism of β-hairpin folding via *f*-value analysis. *Biochemistry 45*, 2668–2678.
10. Du, D., Zhu, Y., Huang, C.-Y., and Gai, F. (2004) Understanding the key factors that control the rate of β-hairpin folding. *Proc. Natl. Acad. Sci. U.S.A. 101*, 15915–15920.
11. Maynard, A. J., Sharman, G. J., and Searle, M. S. (1998) Origin of β-hairpin stability in solution: Structural and thermodynamic analysis of the folding of a model peptide supports hydrophobic stabilization in water. *J. Am. Chem. Soc. 120*, 1996–2007.
12. Muñoz, V., Henry, E. R., Hofrichter, J., and Eaton, W. A. (1998) A statistical mechanical model for β-hairpin kinetics. *Proc. Natl. Acad. Sci. U.S.A. 95*, 5872–5879.
13. Searle, M. S., Zerella, R., Williams, D. H., and Packman, L. C. (1996) Native-like β-hairpin structure in an isolated fragment from ferredoxin: NMR and CD studies of solvent effects on the N-terminal 20 residues. *Protein Eng. 9*, 559–565.
14. Smith, A. W., Chung, H. S., Ganim, Z., and Tokmakoff, A. (2005) Residual native structure in a thermally denatured β-hairpin. *J. Phys. Chem. B 109*, 17025–17027.
15. Smith, A. W., and Tokmakoff, A. (2007) Amide I two-dimensional infrared spectroscopy of β-hairpin peptides. *J. Chem. Phys. 126*, 045109/1–045109/11.
16. Smith, A. W., and Tokmakoff, A. (2007) Probing local structural events in β-hairpin unfolding with transient nonlinear infrared spectroscopy. *Angew. Chem., Int. Ed. 46*, 7984–7987.
17. Hauser, K., Krejtschi, C., Huang, R., Wu, L., and Keiderling, T. A. (2008) Site-specific relaxation kinetics of a tryptophan zipper hairpin peptide using temperature-jump IR-spectroscopy and isotopic labeling. *J. Am. Chem. Soc. 130*, 2984–2992.
18. Hilario, J., Kubelka, J., and Keiderling, T. A. (2003) Optical Spectroscopic Investigations of Model β-Sheet Hairpins in Aqueous Solution. *J. Am. Chem. Soc. 125*, 7562–7574.
19. Honda, S., Kobayashi, N., and Munekata, E. (2000) Thermodynamics of a β-hairpin structure: Evidence for cooperative formation of folding nucleus. *J. Mol. Biol. 295*, 269–278.
20. Setnicka, V., Huang, R., Thomas, C. L., Etienne, M. A., Kubelka, J., Hammer, R. P., and Keiderling, T. A. (2005) IR Study of Cross-Strand Coupling in a β-Hairpin Peptide Using Isotopic Labels. *J. Am. Chem. Soc. 127*, 4992–4993.
21. Huang, R. (2007) Infrared and circular dichroism studies of carbon-13 isotopically labeled peptide models. Ph.D. Thesis, University of Illinois, Chicago.
22. Huang, R., Kubelka, J., Barber-Armstrong, W., Silva, R. A. G. D., Decatur, S. M., and Keiderling, T. A. (2004) Nature of Vibrational Coupling in Helical Peptides: An Isotopic Labeling Study. *J. Am. Chem. Soc. 126*, 2346–2354.
23. Huang, R., Setnicka, V., Etienne, M. A., Kim, J., Kubelka, J., Hammer, R. P., and Keiderling, T. A. (2007) Cross-strand coupling of a β-hairpin peptide stabilized with an Aib-Gly turn using isotope-edited IR spectroscopy. *J. Am. Chem. Soc. 129*, 13592–13603.
24. Huang, R., Wu, L., McElheny, D., Bour, P., and Keiderling, T. A. (2009)Cross-strand coupling and site-specific unfolding thermodynamics of a Trpzip hairpin peptide using ^{13}C isotope labeling and IR spectroscopy (submitted for publication).
25. Kobayashi, N., Honda, S., Yoshii, H., and Munekata, E. (2000) Role of side-chains in the cooperative β-hairpin folding of the short C-terminal fragment derived from streptococcal protein G. *Biochemistry 39*, 6564–6571.
26. Santoveri, C. M., Santoro, J., Rico, M., and Jimenez, M. A. (2002) Thermodynamic analysis of β-hairpin-forming peptides from the thermal dependence of ^{1}H NMR chemical shifts. *J. Am. Chem. Soc. 124*, 14903–14909.
27. Snow, C. D., Qiu, L., Du, D., Gai, F., Hagen, S. J., and Pande, V. S. (2004) Trp zipper folding kinetics by molecular dynamics and temperature-jump spectroscopy. *Proc. Natl. Acad. Sci. U.S.A. 101*, 4077–4082.
28. Wang, T., Xu, Y., Du, D., and Gai, F. (2004) Determining β-sheet stability by Fourier transform infrared difference spectra. *Biopolymers 75*, 163–172.
29. Wang, J., Chen, J., and Hochstrasser, R. M. (2006) Local structure of β-hairpin isotopomers by FTIR, 2D IR, and Ab initio theory. *J. Phys. Chem. B 110*, 7545–7555.
30. Yang, W.-Y., Pitera, J. W., Swope, W. C., and Gruebele, M. (2004) Heterogeneous Folding of the trpzip Hairpin: Full Atom Simulation and Experiment. *J. Mol. Biol. 336*, 241–251.
31. Zhang, J., Qin, M., and Wang, W. (2006) Folding mechanism of β-hairpin studied by replica exchange molecular simulations. *Proteins: Struct., Funct., Bioinf. 62*, 672–685.
32. Cochran, A. G., Skelton, N. J., and Starovasnik, M. A. (2001) Tryptophan zippers: Stable, monomeric β-hairpins. *Proc. Natl. Acad. Sci. U.S.A. 98*, 5578–5583.
33. Cochran, A. G., Skelton, N. J., and Starovasnik, M. A. (2002) correction: Tryptophan zippers: Stable, monomeric β-hairpins. *Proc. Natl. Acad. Sci. U.S.A. 99*, 9081–9082.
34. Cochran, A. G., Tong, R. T., Starovasnik, M. A., Park, E. J., McDowell, R. S., Theaker, J. E., and Skelton, N. J. (2001) A Minimal peptide scaffold for β-turn display: Optimizing a strand position in disulfide-cyclized β-hairpin. *J. Am. Chem. Soc. 123*, 625–632.
35. Russell, S. J., Blandl, T., Skelton, N. J., and Cochran, A. G. (2003) Stability of cyclic β-hairpin: Asymmetric contributions from side chains of a hydrogen-bonded cross-strand residue pair. *J. Am. Chem. Soc. 125*, 388–395.
36. Russell, S. J., and Cochran, A. G. (2000) Designing stable β-hairpins: Energetic contribution from cross-strand residues. *J. Am. Chem. Soc. 122*, 12600–12601.
37. Kiehna, S. E., and Waters, M. L. (2003) Sequence dependence of β-hairpin structure: Comparison of a salt bridge and an aromatic interaction. *Protein Sci. 12*, 2657–2667.
38. Tatko, C. D., and Waters, M. L. (2002) Selective Aromatic Interactions in β-Hairpin Peptides. *J. Am. Chem. Soc. 124*, 9372–9373.
39. Roy, A., Bour, P., and Keiderling, T. A. (2009) Time dependent density functional simulation of the electronic circular dichroism of Trpzip peptides (manuscript to be submitted for publication).
40. Wu, L., Huang, R., and Keiderling, T. A. (2009) Role of hydrophobic interactions and turn stability in β-hairpin conformation studied by optical spectroscopy (manuscript to be submitted for publication).
41. Harada, I., Miura, T., and Takeuchi, H. (1986) Origin of the doublet at 1360 and 1340 cm^{-1} in the Raman spectra of tryptophan and related compounds. *Spectrochim. Acta 42A*, 307–312.
42. Takeuchi, H. (2003) Raman structural markers of tryptophan and histidine side chains in proteins. *Biopolymers 72*, 305–317.
43. Takeuchi, H., and Harada, I. (1986) Normal coordinate analysis of the indole ring. *Spectrochim. Acta 42A*, 1069–1078.

44. Bandekar, J. (1992) Amide modes and protein conformation. *Biochim. Biophys. Acta 1120*, 123–143.
45. Krimm, S., and Bandekar, J. (1986) Vibrational spectroscopy and conformation of peptides, polypeptides, and proteins. *Adv. Protein Chem. 38*, 181–364.
46. Surewicz, W. K., Mantsch, H. H., and Chapman, D. (1993) Determination of protein secondatry structure by Fourier transform infrared spectroscopy: A critical assessment. *Biochemistry 32*, 389–394.
47. Keiderling, T. A., and Silva, R. A. G. D. (2002) Conformational studies using infrared techniques. In *Synthesis of peptides and peptidomimetics* (Goodman, M., Ed.) Georg Thieme Verlag, Stuttgart, Germany.
48. Haris, P. I. (2000) Fourier Transform Infrared Spectroscopic Studies of Peptides: Potentials and Pitfalls. In *Infrared Analysis of Peptides and Proteins: Principles and Applications. ACS Symposium Series* (Ram Singh, B., Ed.) pp 54−95, American Chemical Society, Washington, DC.
49. Haris, P. I., and Chapman, D. (1995) The conformational analysis of peptides using Fourier Transform IR spectroscopy. *Biopolymers 37*, 251–263.
50. Fink, A. L. (1995) Compact intermediate states in protein folding. *Annu. Rev. Biophys. Biomol. Struct. 24*, 495–522.
51. Surewicz, W. K., and Mantsch, H. H. (1995) Infrared absorption methods for examining protein structure. In *Spectroscopic methods for determining protein structure in solution* (Havel, H. A., Ed.) pp 135−162, VCH Publishers, New York.
52. Harper, J. D., and Lansbury, P. T. (1997) Models of amyloid seeding in Alzheimer's desease and scrapie: Mechanistic truths and physiological consequences of the time-dependent solubility of amyloid proteins. *Annu. Rev. Biochem. 66*, 385–407.
53. Rochet, J. C., and Lansbury, P. T. (2000) Amyloid fibrillogenesis: Themes and variations. *Curr. Opin. Struct. Biol. 10*, 60–68.
54. Kubelka, J., Panscoska, P., and Keiderling, T. A. (1999) Novel use of a static modification of two-dimensional correlation analysis. Part II: Hetero-spectral correlations of protein Raman, FT-IR, and circular dichroism. *Appl. Spectrosc. 53*, 666–671.
55. Wang, Z., Tibudan, M., and Keiderling, T. A. (2008) SERS-based Biosensors using Gold Nanoparticles, in *Proceedings of the XXIst International Conference on Raman Spectroscopy* (Withnall, R., and Chowdhry, B. Z., Eds.) pp 484−485, IMPublications, Chichester, U.K.
56. Dempsey, C. E., Mason, P. E., Brady, J. W., and Neilson, G. W. (2007) The reversal by sulfate of the denaturant activity of guanidium. *J. Am. Chem. Soc. 129*, 15895–15902.
57. Rava, R. P., and Spiro, T. G. (1985) Ultraviolet resonance Raman spectra of insulin and α-lactalbumin with 218- and 200-nm laser excitation. *Biochemistry 24*, 1861–1865.
58. Fabian, H., Schultz, C., Naumann, D., Landt, O., Hahn, U., and Saenger, W. (1993) Secondary structure and temperature-induced unfolding and refolding of ribonuclease T_1 in aqueous solution. *J. Mol. Biol. 232*, 967–981.
59. Scheyhing, C. H., Meersman, F., Ehrmann, M. A., Heremans, K., and Vogel, R. F. (2002) Temperature-pressure stability of green fluorescent protein: A Fourier transform infrared spectroscopy study. *Biopolymers 65*, 244–253.
60. Fabian, H., Shultz, C., Beckman, J., Hahn, U., Saenger, W., Mantsch, H. H., and Naumann, D. (1994) Impact of point mutations on the structure and thermal stability of ribonuclease T_1 in aqueous solution probed by Fourier transform infrared spectroscopy. *Biochemistry 33*, 10725–10730.
61. Blanco, F. J., and Serrano, L. (1995) Folding of protein G B1 domain studied by the conformational characterization of fragments comprising its secondary structure elements. *Eur. J. Biochem. 230*, 634–649.
62. Pastor, M. T., Gimenez-Giner, A., and Perez-Paya, E. (2005) The role of an aliphatic-aromatic interaction in the stabilization of a model β-hairpin peptide. *ChemBioChem 6*, 1753–1756.
63. Cooper, W. J., and Waters, M. L. (2006) Model systems for 102-hairpin and β-sheet. *Curr. Opin. Struct. Biol. 16*, 514–524.
64. Fersht, A. R., Shi, J. P., Knill-Jones, J., Lowe, D. M., Wilkinson, A. J., Blow, D. M., Brick, P., Carter, P., Waye, M. M. Y., and Winter, G. (1985) Hydrogen bonding and biological specificity analyzed by protein engineering. *Nature 314*, 235–238.
65. Sheu, S. Y., Yang, D. Y., Selzle, H. L., and Schlag, E. W. (2003) Energetics of hydrogen bonds in peptides. *Proc. Natl. Acad. Sci. U.S.A. 100*, 12683–12687.
66. Williams, D. H., Searle, M. S., Mackay, J. P., Gerhard, U., and Maplestone, R. A. (1993) Toward an estimation of binding constants in aqueous solution: Studies of associations of vancomycin group antiboiotics. *Proc. Natl. Acad. Sci. U.S.A. 90*, 1172–1178.
67. Zagrovic, B., Snow, C. D., Khaliq, S., Shirts, M. R., and Pande, V. S. (2002) Native-like mean structure in the unfolded emsemble of small proteins. *J. Mol. Biol. 323*, 153–164.
68. Ianoul, A., Mikhonin, A., Lednev, I. K., and Asher, S. A. (2002) UV resonance Raman study of the spatial dependence of α-helix unfolding. *J. Phys. Chem. A 106*, 3621–3624.
69. Lopez, M. M., Chin, D.-H., Baldwin, R. L., and Makhatadze, G. I. (2002) The enthalpy of the alanine peptide helix measured by isothermal titration calorimetry using metal-binding to induce helix formation. *Proc. Natl. Acad. Sci. U.S.A. 99*, 1298–1302.
70. Luo, P., and Baldwin, R. L. (1997) Mechanism of helix introduction by trifluoroethanol: A framework for extrapolating the helix-forming properties of peptides from trifluoroethanol/water mixtures back to water. *Biochemistry 36*, 8413–8421.
71. Luo, P., and Baldwin, R. L. (1999) Interaction between water and polar group of the helix backbone: An important determinant of helix propensities. *Proc. Natl. Acad. Sci. U.S.A. 96*, 4930–4935.
72. Scholtz, J. M., Marqusee, S., Baldwin, R. L., York, E. J., Stewart, J. M., Santoro, M., and Bolen, D. W. (1991) Calorimetric determination of the enthalpy change for the α helix to coil transition of an alanine peptide in water. *Proc. Natl. Acad. Sci. U.S.A. 88*, 2854–2858.
73. Privalov, P. L., and Gill, S. J. (1986) Stability of protein structure and hydrophobic interaction. *Adv. Protein Chem. 39*, 191–234.

BI8019838